Egy. J. Pure & Appl. Sci. 2022; 60(2):51-67

Egyptian Journal of Pure and Applied Science

Gaseous Plasma's Time-behavior on a Plate Motion Damping with Time Influenced by a Non-Uniform Non-Stationary Electric Field

T. Z. Abdel Wahid [1], M. Kh. Hadhouda [2]

[1] *Mathematics and Computer Science Department, Faculty of Science, Menoufia University, Shebin El-Kom 32511, Egypt.*
[2] *Basic Sciences Department, El Gazeera High Institute for Engineering and Technology, Cairo, Egypt.*

ARTICLE INFO

Received 30 January 2022
Accepted 30 May 2022

Keywords

Gaseous Plasma,
Unsteady analytical solution,
External electric field,
Irreversible non-equilibrium thermodynamics,
Boltzmann Kinetic equation,
Maxwell equations,
Entropy,
Internal energy,
Nonlinear electromagnetic field.

Correspondence

T. Z. Abdel Wahid

E-mail

taha_zakaraia@yahoo.com

ABSTRACT

The research subject is the kinetic and irreversible non-equilibrium thermodynamics (**INTD**) behaviour of gaseous plasma (**GP**) flow limited by a moving rigid flat plate (**RFP**), its motion damping with time. The effects of non-stationary nonlinear applied electric field (**NLAEF**) were examined on the **GP**. To explore **GP** with the electron velocity distribution function (**EVDF**), researchers have concentrated on the Bhatnagar-Gross-Krook (**BGK**)–model of the kinetic Boltzmann equation (**BE**). An analytical solution was found using the moment (**MM**), travelling wave, and shooting method. An interesting comparison between the non-equilibrium **EVDF** and the equilibrium **EVDF** is made carefully in the present and three previous critical studies. We discovered that the **NLAEF** has a significant impact on **GP**. Compared to the influence of the nonlinear applied magnetic field (**NLAMF**), it caused it to vary and disturb substantially. To save the equilibrium state (**ES**) for a **GP**, we need to apply **NLAMF** rather than **NLAEF** in the plasma controlling procedure. Moreover, we found that the oscillating boundaries keep **ES** rather than the moving boundaries in both **NLAEF** and **NLAMF**. We also found that the system goes to **ES** vastly in the case of **NLAMF**. The relations between the variables that participated in internal energy modifications (**IEM**) are examined. The importance of this research stems from its wide applications in domains such as physics, electrical engineering, micro-electro-mechanical systems (**MEMS**), and nano-electro-mechanical systems (**NEMS**) technologies in industrial and commercial sectors.

1. Introduction

In the MEMS industries, BE provides numerous advantages. Because their micron-scale size is ordinarily relative to the molecule mean free path under typical operating settings, one of the numerous essential issues leading to the use of BE in MEMS and NEMS performances is the awareness that: As a result, in MEMS and NEMS, the Knudsen flow values are frequently distant from the continuum rules. The word "microflow" describes flow on a micron size. In microflows, flow gradient lengths are typically modest and resemble the molecules' mean free path. MEMS and NEMS typically have lengths in the micron range or more minor, resulting in Knudsen numbers ranging from 0.001 to 10. Low-temperature GP or vacuum GP technologies have been widely used in semiconducting and circuit boards for over five decades. They are widely used in magnetic media, metal processing, and cleaning, including carbon removal after laser cutting. These systems achieve new industrial implementations in microelectronics and photonics by reengineering the surface

characteristics of polypropylene. That permits such manufacturers to modify the physicochemical characteristics of the material's surface without influencing the properties of the entire material [1-4]. The temperature, T_α, of low-temperature plasmas, may be characterized as $T_i \approx T_n \approx T_e$, where T_i is ions temperature, T_e is electrons temperature, and T_n is neutral atom temperature. These characteristics help create GP-based technology that employs various electron and ion MVDFs. They characterize the kinetic behaviour of the GP by conveying the energy accessible to a large variety over multiple collisional phenomena. As a result, it is critical to compare the electrons' EVDF with the ES and modify it to follow the electron behaviour. It is generally known that the BE is often used to characterize GP mobility in compressional GP when microscopic factors are considered. Many analytical and experimental contributions [6], [7] are concerned with creating approaches for obtaining realistic solutions to BE. BGK-type [8-10] is the most impressive approximation of the difficult collision factor in BE. As a result, various trials employing MM [11]-[12] have been established to handle the BE depending on the BGK-type.

Greater mean free path values sufficiently explained the rarefied gases for ionized flows throughout various Knudsen numbers (***Kn* ~ 0.1-10**). Modified amounts of the recognized size in MEMS and NEMS technologies are widely utilized in various commercial activities (see Refs. [11-15]). In GP technology, particularly in low-temperature GP, the contact between flowing GP and rigid surfaces is critical. The ionization degree of charged particles is modest, with a single charged particle having between 100,000 and 1,000,000 neutrals. As a result, instability, discharge management, and the creation of excited atoms are all handled by ions.

For example, Ref. [15] investigates the flow dynamics of GP over RFPs using the BE. Furthermore, [16]-[29] have investigated GP's various flows. They used a numerical solution of the collision frequencies to characterize the behaviour of the charged particle. **Yan** [30] presented a Hybrid methodology combining Monte Carlo, Particles in Cell, and Macro-Micro decomposed techniques. **Pan *et al.*** [31] examined the possibility of gas EVDF in discontinuous speed space utilizing the finite volume approach, using GP transportation in the accelerating electric term of the BGK-model.

Juno *et al.* [32] used finite elements and Runge–Kutta algorithms to examine a novel method for 6D GP to discretize the Vlasov–Maxwell system to find new EVDF alternatives. Using a preservation kinetic gas method, **Liu *et al.*** [33] devised a new approach for GP flow problems with large *Kn* and Debye length quantities. Now we are looking into the influence of electron-ion-neutral collisions in the BGK-kind and then calculating the exact solutions for the problem. Furthermore, we handle the entire BGK-kind collision frequency to prevent model discontinuities without any cut-off based on the total values of the independent variable [16]-[29]. The structure of equations was explained with several assumptions in these studies.

The BE's improvement allows us to examine the concepts of INTD. According to research findings, the displacement current associated with the NLAEF could not be negated in the problem therapy. The non-stationary oscillating flow is studied by **Wahid *et al.*** [34] in an INTD environment utilizing the Stokes problem. Under the NLAEF effect, we wanted to employ GP simulation next to a limitless oscillating RFP. The BGK-kind model was combined with the ME model. Furthermore, two-sided MVDFs were used with **MM** and travelling wave solutions.

Finally, theoretical descriptions of thermodynamic and electromagnetic variables were provided. The difference in variation amongst the MVDFs and the perturbed MVDFs is shown. Because of the BE's characteristics, we investigate INTD concepts. The findings are in good accord with those found in [34].

2. GEOMETRY AND GOVERNING EQUATIONS OF THE PROBLEM

Analyzing a GP helium system with an unsteady NLAEF, E_{xA} parallel to flow path positioned near an infinite horizontally RFP $y= 0$, bordered by the upper half-space at $y \geq 0, see$ Fig. 1. Initially, GP is contained in an ES. It gets hypothesized that the GP is isothermal $T_e \approx T_i$ and quasi-neutral. We indicate the NLAEF direction on the x-axis and the induced magnetic field on the z-axis. GP flows to an unstable NLAEF, and the surface RFP moves with a velocity equal to $V_0 e^{-\omega t}$ along the x-axis. Furthermore, the reflected particles acquired RFP velocity in every case.

Lorentz force $\vec{F}_e$ which is behaving, at a constant temperature, on electrons and ions

$$\vec{F}_e = -e\vec{E} - \frac{e}{c}(\vec{\eta} \wedge \vec{B}), \quad \text{here} \quad \vec{E} = E_x\vec{\imath} = (E_{xA} + E_{xi})\vec{\imath}, as\ E_{xA} = E_0 e^{\phi_0(k_1 y + k_2 t + k_0)} \qquad (1)$$

The applied non-uniform unstable electric field and the induced one are represented by E_{xA} and E_{xi}, respectively, and the k_0, k_1, and k_2 constants have restricted values to prevent the electric field from diverging.

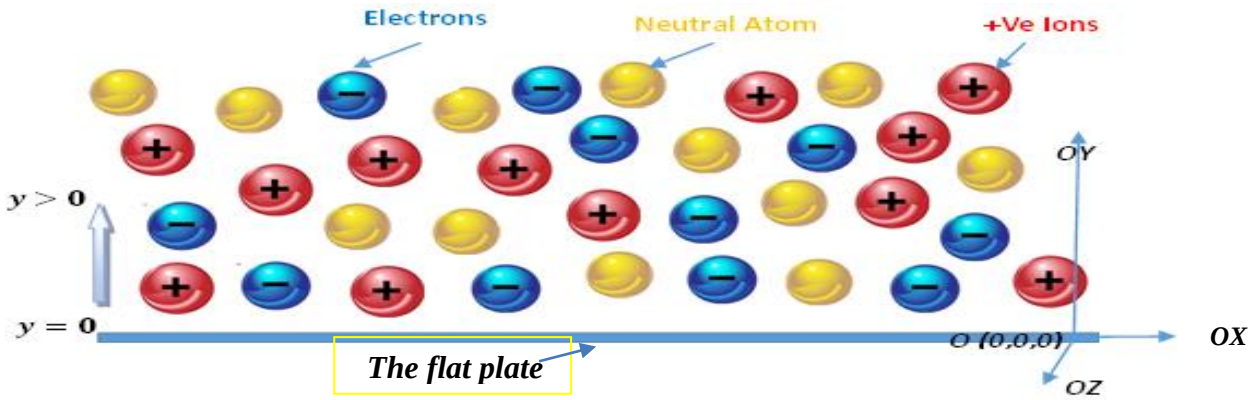

Fig. 1 Schematic representation of our problem. The rigid flat plate located at $y = 0$ and the plasma components occupied the half-space $y > 0$

The ME equations are satisfied and can be represented as [7]:

$\vec{V} \equiv (V_x, 0,0), \vec{J} \equiv (qnV_x, 0,0), \vec{E} \equiv (E_x, 0,0)$ and $\vec{B} \equiv (0,0,B_z)$ (2)

Using the kinetic characterization of GP, the electrons EVDF $g_e(\vec{r},\vec{\eta},t)$ linked to helium-GP can be examined theoretically. We analyze the well-known BE-like kinetic equation with a collision term of the BGK-model, which reproductions the EVDF [36]:

$$\frac{\partial g_e(\vec{r},\vec{\eta},t)}{\partial t} + \vec{\eta}\cdot\frac{\partial g_e}{\partial \vec{r}} + \frac{\vec{F}_e}{m_e}\cdot\frac{\partial g_e}{\partial \vec{\eta}} = \omega_{ee}(g_{0e} - g_e) + \omega_{ei}(g_{0i} - g_e) + \omega_{en}(g_{0n} - g_e)\ as\ g_{0\alpha} = n_\alpha(2\pi RT_\alpha)^{-\frac{3}{2}} e^{\frac{-(\vec{\eta}-\vec{V}_\alpha)^2}{2RT_\alpha}} \quad (3)$$

The variables $n_\alpha, \vec{V}_\alpha$, and T_α, distinguish the significant characteristics of the model can be obtained using **MM**. The beginning and boundary conditions can be represented as [16, 17, 29, 46] based on the geometry of the issue:

$V_{x2}(0,t) = V_0 e^{-\omega t}$ at $t > 0$, V_x is finite at $y \to \infty$, and $V_x = V_{x2}$ at $\eta_y > 0$.

These hypotheses will translate the GP kinetic equation into a proper shape.

$$\frac{\partial g_e}{\partial t} + \eta_y\frac{\partial g_e}{\partial y} - \frac{eB_{ez}}{m_e c}(\eta_y\frac{\partial g_e}{\partial \eta_x} - \eta_x\frac{\partial g_e}{\partial \eta_y}) + \frac{eE_{ex}}{m_e}\frac{\partial g_e}{\partial \eta_x} = \omega_{ee}(g_{0e} - g_e) + \omega_{ei}(g_{0i} - g_e) + \omega_{en}(g_{0n} - g_e) \quad (4)$$

ω_{ee}, ω_{ei}, and ω_{en} collision frequencies take the form [37, 38]:

$$\omega_{ee} = \left(\frac{4\sqrt{\pi}n_e e^4 Log[\Lambda_{ee}]}{3\sqrt{m_e}K_B^{\frac{3}{2}}T_e^{\frac{3}{2}}}\right), \omega_{ei} = \left(\frac{4\sqrt{2\pi}n_i e^4 Z^2 Log[\Lambda_{ei}]}{3\sqrt{m_e}K_B^{\frac{3}{2}}T_e^{\frac{3}{2}}}\right), \omega_{en} = \left(\frac{4\sqrt{\pi m_n}n_e e^4 Log[\Lambda_{en}]}{3m_e K_B^{\frac{3}{2}}T_e^{\frac{3}{2}}}\right) \quad (5)$$

Here, $\lambda_{De} = \lambda_{Di} = \lambda_D$, $Log[\Lambda] = Log[4\pi n\lambda^3{}_D]$, and Z are Debye lengths, Coulomb logarithm, and ionization degree.

Lee's approach to inherently unknowable functions of time and space, V_{x1} and V_{x2} [38, 39], can be used to solve Eq. (4):

$$g = \begin{cases} g_1 = n(2\pi RT)^{-\frac{3}{2}}\left(1 + \frac{\eta_x V_{x1}}{RT}\right)e^{\left(\frac{-\eta^2}{2RT}\right)} & \text{for } \eta_y < 0 \downarrow, \\ g_2 = n(2\pi RT)^{-\frac{3}{2}}\left(1 + \frac{\eta_x V_{x2}}{RT}\right)e^{\left(\frac{-\eta^2}{2RT}\right)} & \text{for } \eta_y > 0 \uparrow \end{cases} \quad (6)$$

Utilizing Grad **MM** with Eq. (4), we acquire the transfer equations [6]:

$$\frac{\partial}{\partial t}\int \vartheta_j g_e d\underline{\eta} + \frac{\partial}{\partial y}\int \eta_y\vartheta_j g_e d\underline{\eta} + \frac{eE_{xe}}{m_e}\int g_e\frac{\partial \vartheta_j}{\partial \eta_x}d\underline{\eta} - \frac{eB_{ze}}{m_e c}\int(\eta_x\frac{\partial \vartheta_j}{\partial \eta_y} - \eta_y\frac{\partial \vartheta_j}{\partial \eta_x})d\underline{\eta} = \omega_{ee}\int \vartheta_j(g_{0e} - g_e)d\underline{\eta} + \omega_{ei}\int \vartheta_j(g_{0i} - g_e)\,d\underline{\eta} + \omega_{en}\int \vartheta_j(g_{0n} - g_e)d\underline{\eta} \quad (7)$$

The corresponding formula of the functions $\vartheta_j(\vec{\eta})$ integrals over $d\underline{\eta} = d\eta_x d\eta_y d\eta_z$,

$$\int \vartheta_j(\vec{\eta})g\,d\underline{\eta} = \int_{-\infty}^{\infty}\int_{-\infty}^{0}\int_{-\infty}^{\infty}\vartheta_j g_1 d\underline{\eta} + \int_{-\infty}^{\infty}\int_{0}^{\infty}\int_{-\infty}^{\infty}\vartheta_j g_2 d\underline{\eta} \quad (8)$$

The ME can be stated as:

$$\frac{\partial E_{xe}}{\partial y}-\frac{1}{c}\frac{\partial B_{ze}}{\partial t}=0, \quad (9)$$

$$\frac{\partial B_{ze}}{\partial y}-\frac{1}{c}\frac{\partial E_{xe}}{\partial t}-\frac{4\pi e n_e}{c}V_{xe}=0. \quad (10)$$

Observe that the current displacement component in the **ME** is factored into the equation, although in prior research, it was omitted; see [17, 20, 26, 28].

The electromagnetic fields can be computed using the standard forms.

$E_x(y,0)=E_0, B_z(y,0)=0, E_x$ and B_z are finite at y → ∞. (11)

The non-dimensional variables can now be defined as follows:

$$t=t^*\tau_{ee}\,, y=y^*(\tau_{ee}V_{Th})\,, V_x=V_x^*V_{Th}\,, \tau_{xy}=\tau_{xy}^*V_{Th}\,, M=\frac{V_0}{V_{Th}}, E_x=E_x^*\left(\frac{m_e c}{e\tau_{ee}}\right)\,,$$

$$B_z=B_z^*\left(\frac{m_e c}{e\tau_{ee}}\right), \gamma=\frac{m_e}{m_i}, dU=dU^*(K_BT_e) \text{and } g_l=g_l^* n_e(2\pi RT_e)^{-\frac{3}{2}}, l=0,1,2,$$

$$V_{Th}=\sqrt{2RT}, \omega=\frac{\omega^*}{\tau_{ee}}. \quad (12)$$

Mean velocity and shear stress are [38]:

$$V_x=\frac{1}{2}(V_{x1}+V_{x2}), \tau_{xy}=\frac{P_{xy}}{\rho V_0\sqrt{RT_e/2\pi}}=(V_{x2}-V_{x1}). \text{Here} P_{xy}=m\int(\eta_x-V_x)\eta_y g d\underline{\eta} \quad (13)$$

The Mach number (*M=0.01*), so the modification n and T is negligible and $n_\alpha=1+O(M^2)$ and $T_\alpha=1+O(M^2)$. Applying the non-dimensional values and this hypothesis (12) along with $\vartheta_1=\eta_x$ and $\vartheta_2=\eta_x\eta_y$ Eq. (7) will be:

$$\frac{\partial V_{ex}^*}{\partial t^*}+\frac{\partial \tau_{exy}^*}{\partial y^*}-E_{ex}^*=0 \quad (14)$$

$$\frac{\partial \tau_{exy}^*}{\partial t^*}+2\pi\frac{\partial V_{ex}^*}{\partial y^*}+\tau_{exy}^*=0 \quad (15)$$

In this scenario, the initials and boundary conditions will be:

$$\left.\begin{array}{c} V_{ex}^*(y^*,0)=\tau_{exy}^*(y^*,0)=0, \\ 2V_{ex}^*(0,t^*)+\tau_{ex}^*(0,t^*)=2Me^{-\omega^* t^*} \\ V_{ex}^* \text{ and } \tau_{exy}^* \text{ are finite as y} \to \infty. \end{array}\right\} \quad (16)$$

3. METHOD OF SOLUTION FOR THE NONDIMENSIONALIZED SYSTEM

The boundary value issue for electrons will be simplified by removing the star from the non-dimensional parameters.

$$\frac{\partial V_{ex}}{\partial t}+\frac{\partial \tau_{exy}}{\partial y}-E_{ex}=0, \quad (17)$$

$$\frac{\partial \tau_{exy}}{\partial t}+2\pi\frac{\partial V_{ex}}{\partial y}+\left(1+\frac{\omega_{ei}}{\omega_{ee}}+\frac{\omega_{en}}{\omega_{ee}}\right)\tau_{exy}=0, \quad (18)$$

$$\frac{\partial E_{ex}}{\partial y}-\frac{\partial B_{ez}}{\partial t}=0, \quad (19)$$

$$\frac{\partial B_{ez}}{\partial y}-\frac{\partial E_{ex}}{\partial t}-\Omega_{e0}V_{ex}=0. \quad (20)$$

where $\Omega_{e0}=\left(\frac{V_{Th}^2 n_e e^2}{m_e c^2\omega_{ee}^2}\right)$.

Solving BE by applying the travelling wave approach, the electron kinetics be able to be explained in total, and the new item can be represented as follows: [40] - [42]:

$$\gamma=k_1 y+k_2 t+k_0 \quad (21)$$

Here k_1, k_2 and k_0 are constants.

Partial derivatives of Eqs. (17)- (20) can be defined as of Eq. (21):

$$\frac{\partial}{\partial t}=k_2\frac{\partial}{\partial\gamma}\,, \frac{\partial}{\partial y}=k_1\frac{\partial}{\partial\gamma}, \frac{\partial^n}{\partial t^n}=k_2^n\frac{\partial^n}{\partial\gamma^n}\,, \frac{\partial^n}{\partial y^n}=k_1^n\frac{\partial^n}{\partial\gamma^n}. \quad (22)$$

Here n is a positive integral number.

Replacing Eqs. (21)-(22) in Eqs. (17)-(20), we have the next differential equation

$$\left((k_2^2-k_1^2)\left(k_2-\frac{2\pi k_1^2}{k_2}\right)\right)\frac{d^3V_{ex}(\gamma)}{d\gamma^3}+\tau_c(k_2^2-k_1^2)\frac{d^2V_{ex}(\gamma)}{d\gamma^2}-\Omega_{e0}k_2\frac{dV_{ex}(\gamma)}{d\gamma}+\Omega_{e0}\tau_c V_{ex}(\gamma)=0, \tau_c=\left(1+\frac{\omega_{ei}}{\omega_{ee}}+\frac{\omega_{en}}{\omega_{ee}}\right). \quad (23)$$

In its dimensionless form, initial and boundary conditions become:

$$\left\{\begin{array}{c} B_{ez}(\gamma=0)=\tau_{exy}(\gamma=0)=0, E_{ex}(\gamma=0)=E_0; \\ 2\,V_{ex}(\gamma=k_2)+\tau_{exy}(\gamma=k_2)=2Me^{-\omega} \text{ at } y=0 \text{ and } t=1; \\ V_{ex}\,, \tau_{exy}, E_{ex}, \text{ and } B_{ez} \text{ are finite at } \gamma\to-\infty. \end{array}\right. \quad (24)$$

In addition, given Eq. (1), it is observed that, for limited $y>0$ and restricted time intervals, t of applicable concern, the utilized electric field, E_{xE}, stays finite.

Solving the governing equations defining the research lab GP helium using symbolic software (Mathematica).

4. THERMODYNAMIC TREATMENT OF HELIUM-PLASMA MODEL

Examining the INTD features of the GP helium while considering the problem's INTD phenomena. The thermodynamic characteristics of the GP components will be determined by using EVDF in Eq. (6) and ions, electrons, and neutrals collision frequencies. In addition, we will see if our approach is coherent with several thermodynamic principles and the H-theorem for the GP helium. In physics, entropy is derived from INTD. It is one of the state parameters of matter used to characterize how energy is degraded. It refers to a measurement of the status of some material systems in general. The essence of entropy, the degree of internal chaos of a system, is gradually

described with the advent of statistical physics and information theory. Cybernetics, probability theory, life science, and astrophysics are just a few of the domains where it is functional.

4.1. ENTROPY AND ITTS RELATED VARIABLES

According to [16]-[18], [43]: The entropy per unit mass S and its flux have the general structure:

$$S = -\int g_e \ln g_e \, d\underline{\eta} = -\left(\int g_{e1} \ln g_{e1} \, d\underline{\eta} + \int g_{e2} \ln g_{e2} \, d\underline{\eta}\right) = -\pi^{\frac{3}{2}}\left[\left(V_{x1}{}^2 + V_{x2}{}^2\right) - 0.66\right] \quad (25)$$

$$J_y{}^{(S)} = -\int \eta_y g_e \ln g_e \, d\underline{\eta} = -\left(\int \eta_y g_{e1} \ln g_{e1} \, d\underline{\eta} + \int \eta_y g_{e2} \ln g_{e2} \, d\underline{\eta}\right) = \left[\pi\left(V_{x1}{}^2 + V_{x2}{}^2\right)\right]. \quad (26)$$

The entropy production can be calculated when using these principles [16-18, 43]:

$$\sigma = \frac{\partial S}{\partial t} + \vec{\nabla} \bullet \overrightarrow{J^{(S)}} \quad (27)$$

4.2. GIBBS FORMULA AND ITS CONSEQUENCES

Gibbs's formula can calculate the overall system's internal energy modification (IEM) [44]. The two significant types of GP helium magnetization are paramagnetic and diamagnetic. As a result, for both kinds, the total energy alterations can be stated as follows:

IEM in Gibbs' equation is described by the extensive factors *S, P, and B* related to intensive factors *T, E, and* M_B. As a result, the Gibbs law's IEM can be expressed as [29], [44]:

$dU = dU_S + dU_{pol} + dU_{dia}$, such that the IEM as a result of the modification in the entropy is $dU_S = TdS$, the IEM as a result of the modification in polarization is $dU_{pol} = E\,dP$, the IEM as a result of the modification in the magnetic field is $dU_{dia} = -M_B dB$, with $M_B = T\frac{\partial S}{\partial B}$. The IEM in Gibbs' formulation was represented with the extended INTD characteristics *S, P, and M* because of *T, E, and B*, correspondingly. As a result, the Gibbs law's IEM can be expressed as:

$dU = dU_S + dU_{pol} + dU_{par}$. The IEM, as a result of the modification in magnetization, is $dUpara = B\,dM$. Finally, the total IEM as $dU = dS_e + f_1 E_x dp + f_1 B_z dM_B$. That is, in a non-dimensional form formula $dU = dS + Edp - M_B dB$.

5. CALCULATIONS AND RESULTS

This part provides an example of flow in GP [45]. Solving the BGK-kind for GP helium predicated on the INTD utilizing the travelling wave methodology for the ω_{ee}, ω_{ei}, and ω_{en} colliding frequencies, the GP kinetics can be characterized in depth. The findings are displayed in figures and 3D-graph s utilizing a wide variety of standard data for electron gas in GP helium. In the experimental context, the findings in the figures reflect the normal verification consistency between BE and research lab GP estimates [20, 37]. The GP helium loses one electron in the paramagnetic condition. However, the helium-GP loses two electrons due to the atoms' ionizing potential in the diamagnetic scenario. We investigate the accurate values of $k_1, k_2, and\ k_3$ using the idea of the numerical shooting technique obtained $k_1 = 0.83, k_2 = 0.15, k_0 = 0.1$ with the surface Mach number, $M = 10^{-2}$. The problem's computations are performed using various GP parameters and constraints: The electron rest mass and the charge of the electron are $m_e = 9.093 \times 10^{-28} gm, e = 4.8\ 10^{-10} esu.$ Boltzmann's constant, the initial temperature, and the electrons concentration are $k_B = 1.3807 \times 10^{-16}$ erg/K, $T_0 = 300$ K, $n_e = 10^{11}$cm^{-3}. The atom diameter of the helium-GP is $d = 1.4 \times 10^{-8}$cm, and $\Omega_{e0} = 2.9 \times 10^{-6}$. The mean free path is $\lambda = 11.483 \times 10^{3}$cm, which is large compared with the Debye length $\lambda_{De} = 3.779 \times 10^{-4}$ cm. Lastly, ω_{ee}, ω_{ei}, and ω_{en} collision frequencies are $\omega_{ei} = 1.32 \times 10^{9}\, Sec^{-1}$, $\omega_{ee} = 9.34 \times 10^{8}\, Sec^{-1}$,and $\omega_{en} = 2.399 \times 10^{-3} Sec^{-1}$, correspondingly.

It is clear from the behaviours of the EVDF that the ascending particles and their turbulence after colliding with the plate are much more affected than the descending particles that have not yet collided with the plate, see Figs. **2A, 2B**. With the passage of time and the deviation of the system to ES, we find that this disturbance in the behaviours of the particles diminishes little by little; see the gradation and evolution of these behaviours from t = 0.1, 5, 20, 25.9, see Figs. **2A, 2B**. The collision of the ascending turbulent particles with the unperturbed descending particles works to decay these behaviours, seen gradually in Figs. **2A, 2B**. Comparing the EVDF of turbulent electrons and their ES ones shows that this turbulent behaviour is more for the ascending particles than for the descending particles. That is very clear; see Figs. **3A, 3B**.

The first component of the two-branched EVDF of descending particles deduces the tendency to ES much faster than the ascending particles. That is directly affected by the movement of the plate and is also affected by the electromagnetic fields created, which of course, are as strong as possible near the plate forming it, see Figs. **3A, 3B**.

We explore the characteristics of GP in the presence of an applied non-uniform non-stationary electric field that varies in space and time and the impact of identical restrictions. We can study a comparison between different previous studies in Refs. [7, 12, 35].

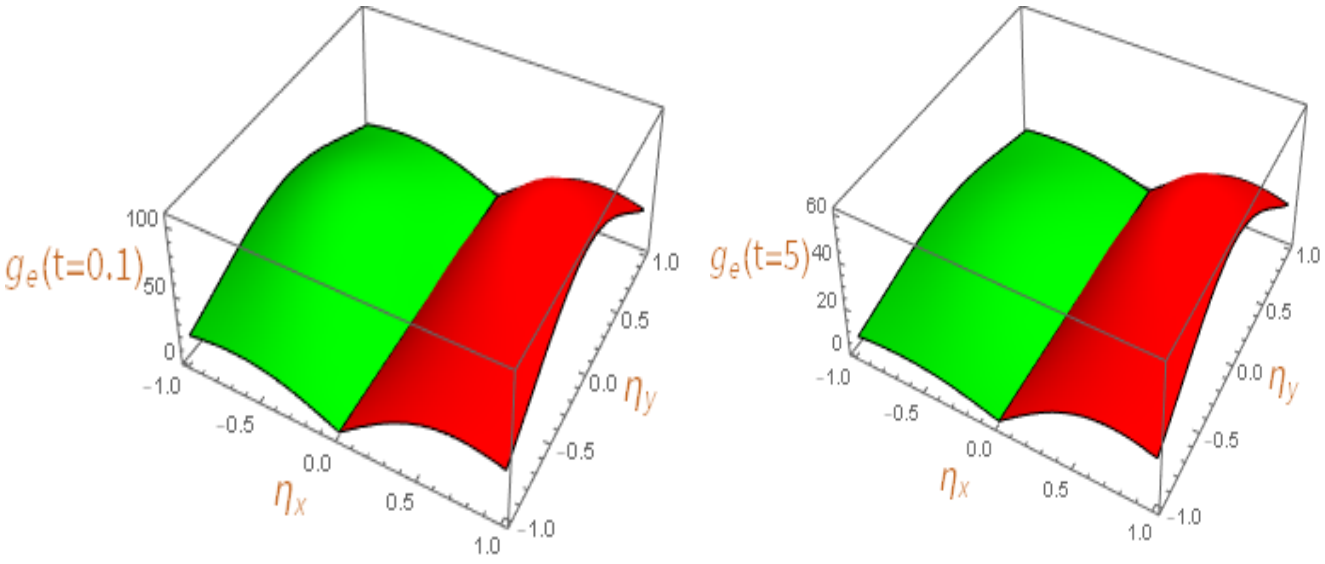

Fig. 2A The disturbed EVDF g_e [g_1 (green), g_2 (red)] at (t = 0.1 and 5) for (y=5) and M = 0.01

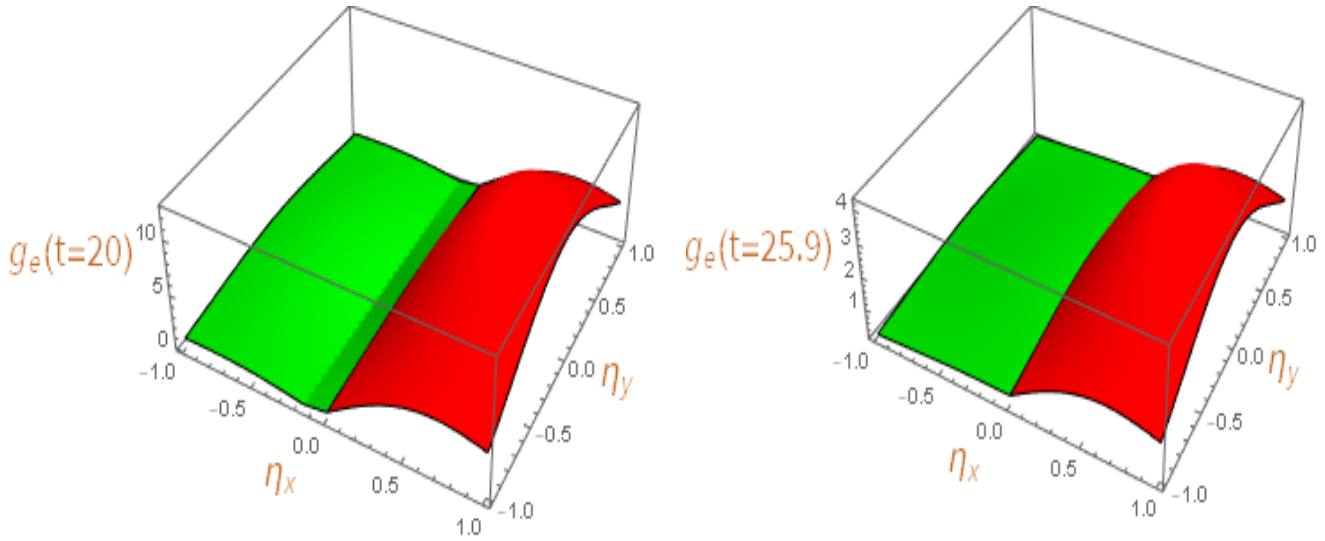

Fig. 2B The disturbed EVDF g_e [g_1 (green), g_2 (red)] at (t = 20 and 25.9) for (y=5) and M = 0.01

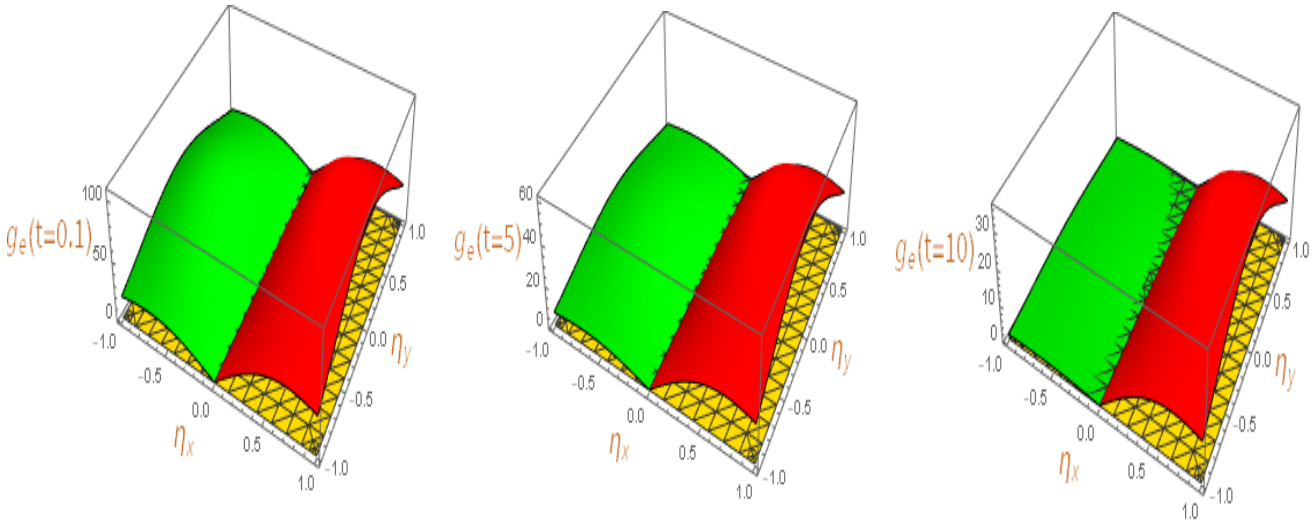

Fig. 3A The pattern of the disturbed EVDF g_e[g_1 (green) and g_2 (red)] contrasted to the balance EVDF g_o (grid) at (t = 0.1, 5 and 10) with M= 0.01 at y=5

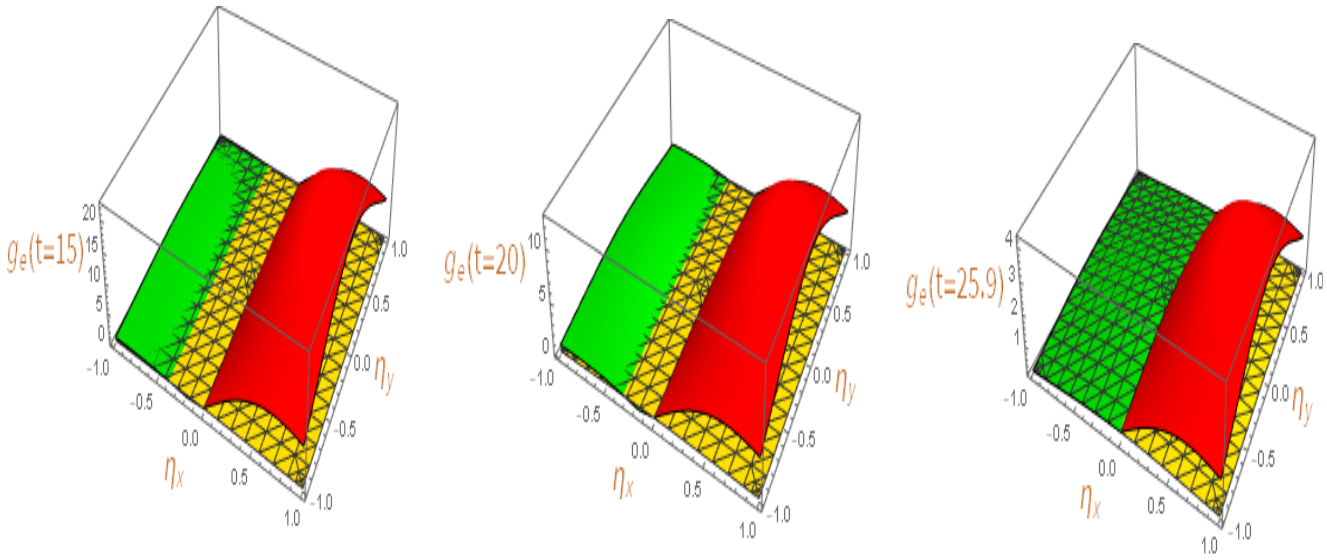

Fig. 3B The pattern of the disturbed EVDF g_e[g_1 (green) and g_2 (red)] contrasted to the balance EVDF g_o (grid) (t = 15, 20, and 25.9) with M= 0.01 at y=5

First comparison: Comparing our Figs. **3-A, B** with the case study in Ref. [12], where NLAMF affected a GP bound by a moving plate. We found that the NLAEF in the case of moving plate has a more substantial influence on EVDF related to GP than the NLAMF compared with Figs. **1-A, B** in Ref. [12], that swiftly drives the GP out of its ES as (*t=2.5*). The EVDF of the GP achieve ES over time, consistent with the laws of INTD as (*t=10*), the GP is a little out of ES owing to NLAEF; see the last 3D-graph of Fig. **1-A**, whereas it has achieved ES owing to NLAEF; check its last 3D-graph of Fig. **1** in Ref. [12]. We find that the NLAEF has a strong effect on GP. When contrasted to the action of the NLAMF, it causes it to vary and perturb aggressively. To keep the ES, we should use the impact of NLAMF rather than the impact of NLAEF in the GP controlling process, which agrees with the same results concluded from the study in Ref. [7].

Second comparison: Comparing our Figs. **3-A, B** with the case study in Ref. [35], where NLAMF affected a GP bounded by an oscillating plate. We found that the NLAEF in the case of moving plate has a more substantial influence on EVDF related to GP than the NLAMF in the case of moving plate compared with Figs. **1-A, B** in Ref. [35], that swiftly drives the GP out of its ES as (*t=5*). The EVDF of the GP achieves ES over time, consistent with the laws of INTD, as (*t=10*), the GP are a little out of ES owing to NLAEF; see the last 3D-graph of Fig. **1-A**, whereas it has achieved ES owing to NLAEF; check its last 3D-graph of Fig. **1** in Ref. [35]. We find that the NLAEF has a strong effect on GP. When contrasted to the action of the NLAMF, it causes it to vary and perturb aggressively. To keep the ES, we should use the impact of NLAMF rather than the impact of NLAEF in the GP controlling process, which agrees with the same results concluded from the study in Ref. [7].

Third comparison: Comparing our Figs. **3-A, B** with the case study in Ref. [35], where NLAEF affected a GP bounded by an oscillating plate. We found that the NLAEF in the case of a moving plate has a more substantial influence on EVDF related to GP than the NLAEF in a case of an oscillating plate compared with Figs. **1-A, B** in Ref. [35].

Figures **4-A, B** show that the NLAEF impacts dramatically raising GP velocity in a short period. That is in harmony with the perturbed EVDF's manner. Away from RFP, the shear stress increases nonlinearly. The shear stress linearly behaves next to the RFP; see Figs **5-A, B**. The NLAMF, on the other hand, behaves nonlinearly, neighbouring to the RFP [35].

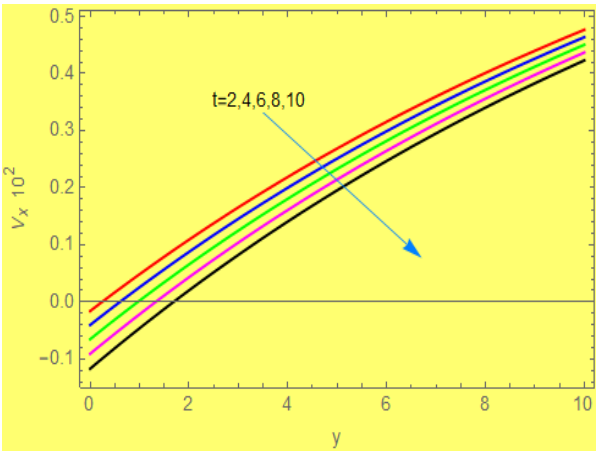

Fig. 4A The profiles of the Velocity V_x

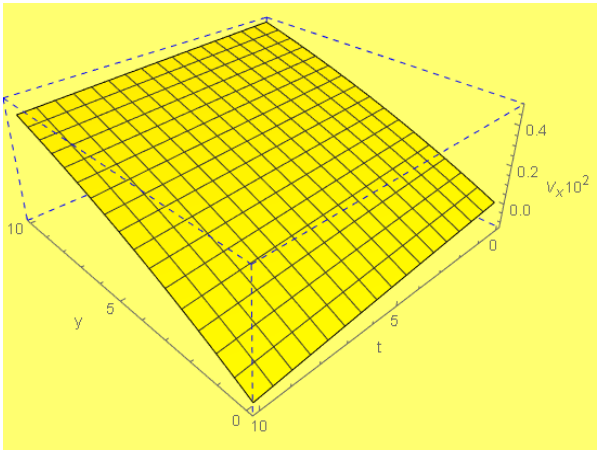

Fig. 4B The Vx Vs y and t

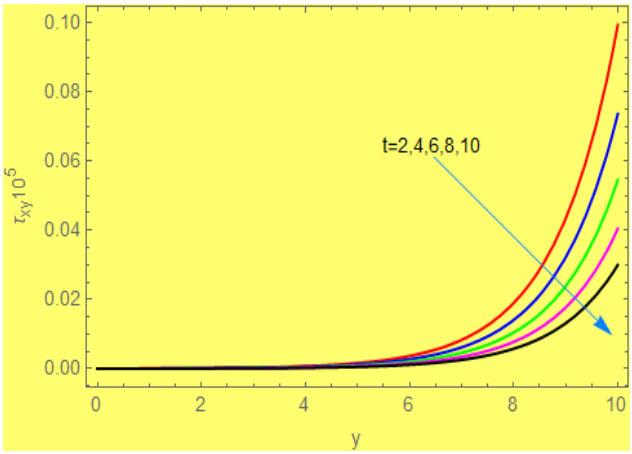

Fig. 5A The profiles of the shear stress τ_{xy}

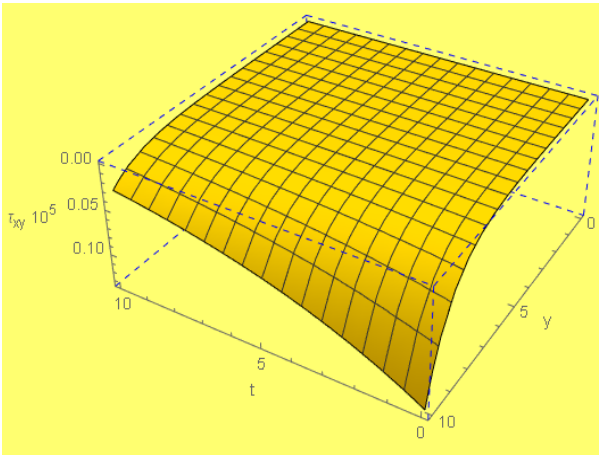

Fig. 5B The τ_{xy} Vs y and t

The viscosity parameter performs in a linear manner neighbouring the surface and in a nonlinear manner far from it; see Figs. **6-A, B**. The NLAMF, on the other hand, behaves in a nonlinear fashion [34]. Figs. **7-A, B** show how the NLAEF's nonlinear acts influence GP and how it is excessive (2×10^3 times) relative to the earlier study's comparable figure; review Fig. **5** in Ref. [35], since it is merely a generated magnetic field formed by RFP motion. It was found to be linked to NLAMF [35].

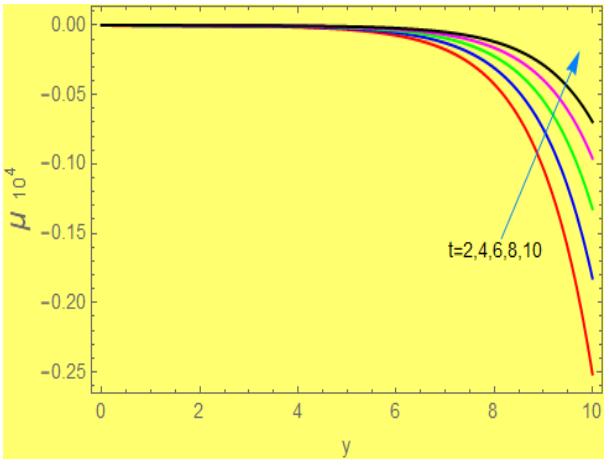

Fig. 6A The profiles of the viscosity coefficient μ

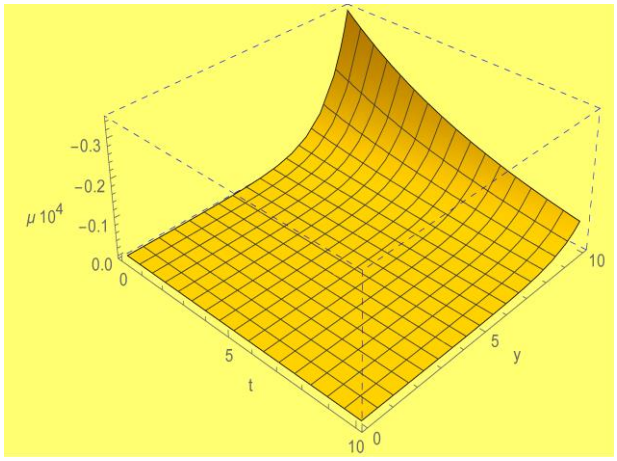

Fig. 6B The μ Vs y and t

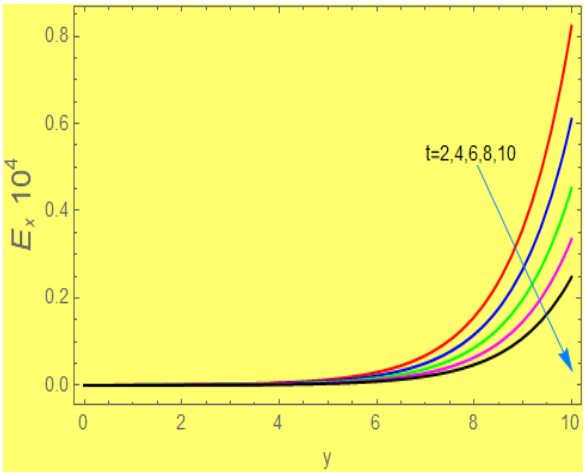

Fig. 7A The profiles of applied electric field Ex

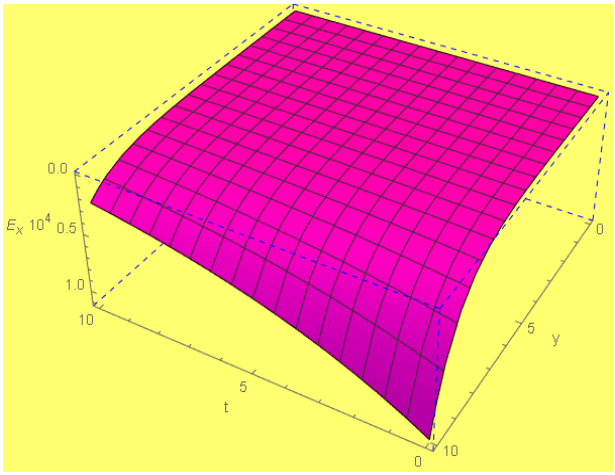

Fig. 7B The Ex Vs y and t

The behaviour of the trustworthy induced magnetic field linked to the NLAEF compared to the NLAMF in [34] is depicted in Figs. **8-A, B**. The fluctuation and perturbation of GP can be explained in this way. When contrasted, a high induced magnetic field is related to the NLAEF, but a small electric field is connected to the NLAMF.

Boltzmann's H-theorem, thermodynamic principles, and Le Chatelier's concept agree that entropy increases with time. It is, however, slow-growing, which justifies the latency of GP electrons reaching an ES in this situation compared to the earlier work [35]; review Figs. **7-A, B**. Compared to the NLAMF [34], we conclude that the pace of reaching an ES in the NLAEF instance is plodding. That supports the hypothesis that employing an NLAMF rather than an NLAEF is optimal for managing electron GP and transferring them to the ES.

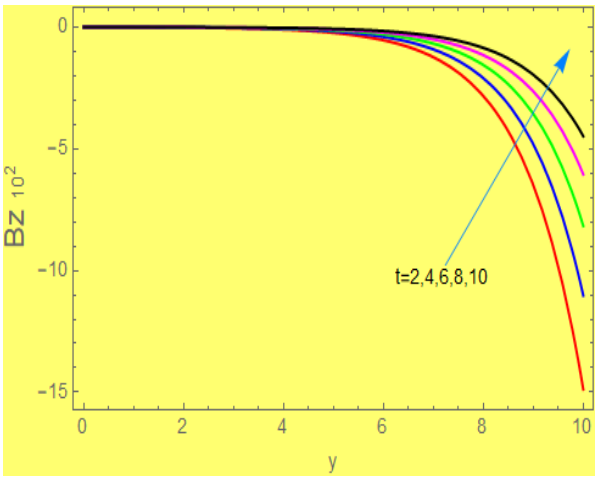

Fig. 8A The profiles of the induced magnetic field Bz

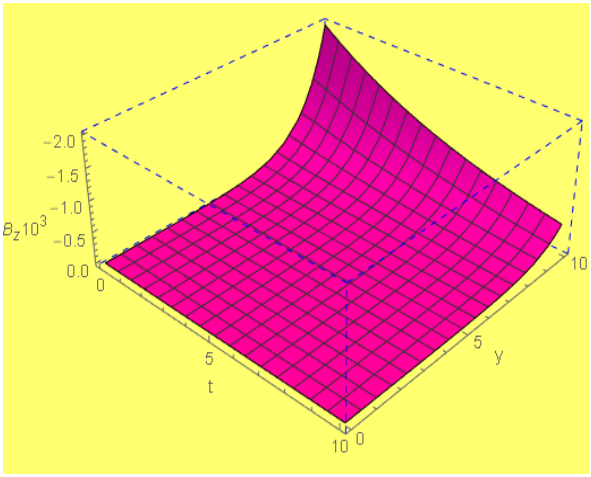

Fig. 8B The Bz Vs y and t

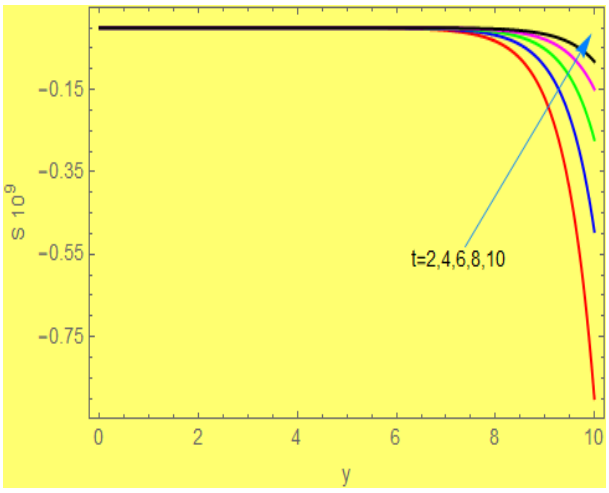

Fig. 9A The profiles of the entropy S

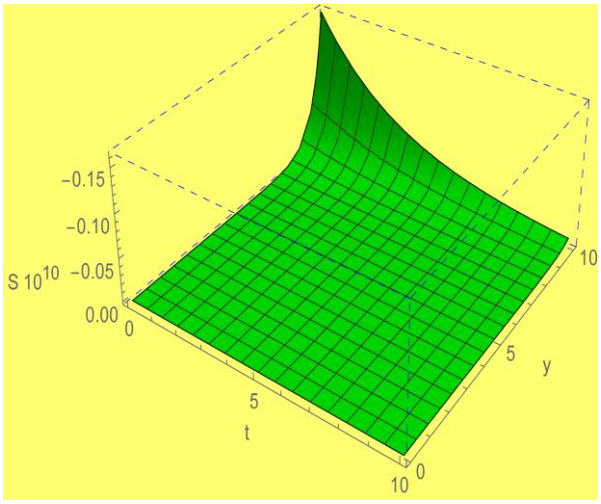

Fig. 9B The S Vs y and t

Entropy generation is a non-negative function for all INTD concepts, as seen in Figures 10-A and B. The IEM is shown in Figs. **(11-A, B), (12-A, B),** and **(13, A, B)** because of multiple factors; this compares in amplitude to the comparable figures in the prior research the following:

$dU_S(NLAMF) : dU_S(NLAEF) = 1 : 10^9$,

$dU_{Pol}(NLAMF) : dU_{Pol}(NLAEF) = 1 : 1.5 \times 10^4$,

$dU_{dia}(NLAMF) : dU_{dia}(NLAEF) = 1 : 2 \times 10^5$.

As shown in [35], the IEM dominates in the NLAEF instance compared to the matching NLAMF cases.

In the case of a research project:

$dU_{Pol} : dU_{dia} : dU_S = 1 : 0.4 \times 10^2 : 1.33 \times 10^5$.

Figs. **14-A, B** show that with NLAEF, the gyrofrequency Ω_c, decreases nonlinearly with space and time, whereas it decreases uniformly with space and time in the Ref. [35]. That is because of the powerful electromagnetic fields occurring in this scenario. Gyro-radius near the solid horizontal RFP shows a substantial perturbation in Figs. **15-A, B**, whereas the NLAMF shows a smooth and consistent variation [35].

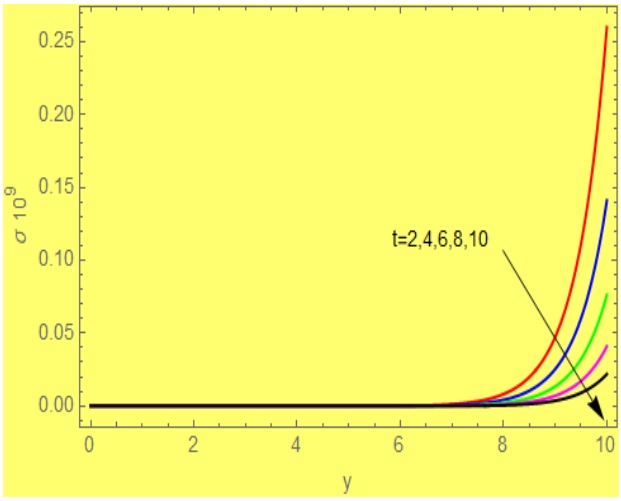

Fig. 10A The profiles of the entropy production σ

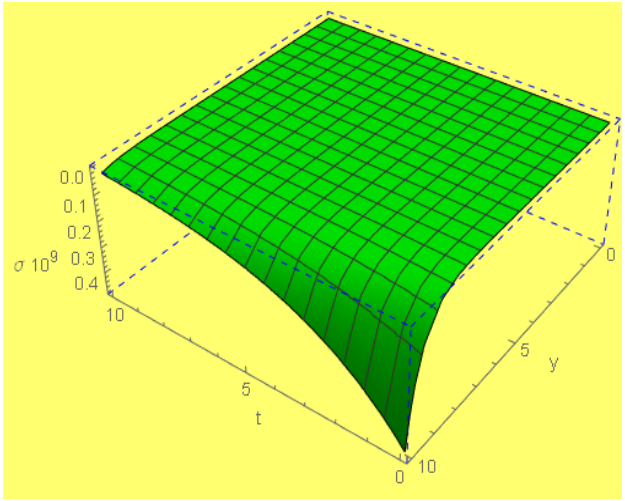

Fig. 10B The σ Vs y and t

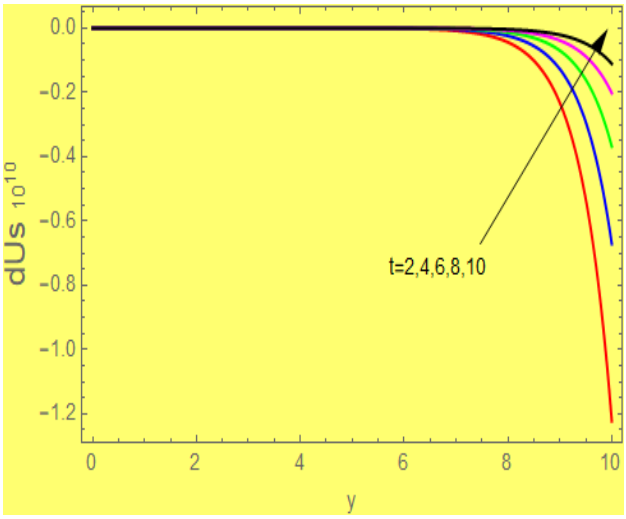

Fig. 11A The profiles of the IEM dU_s

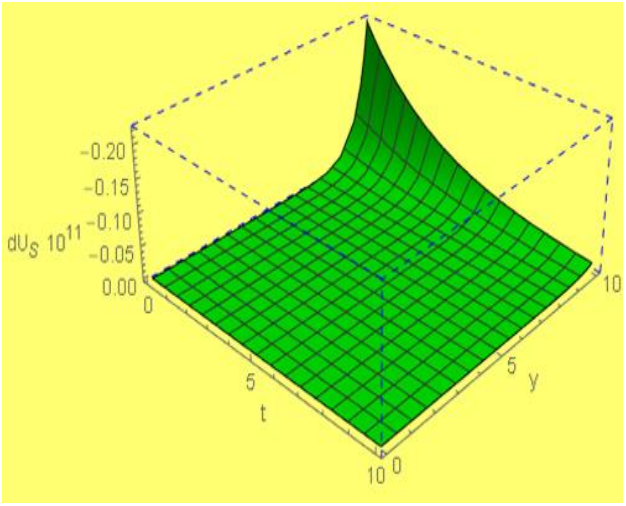

Fig. 11B The dU_s Vs y and t

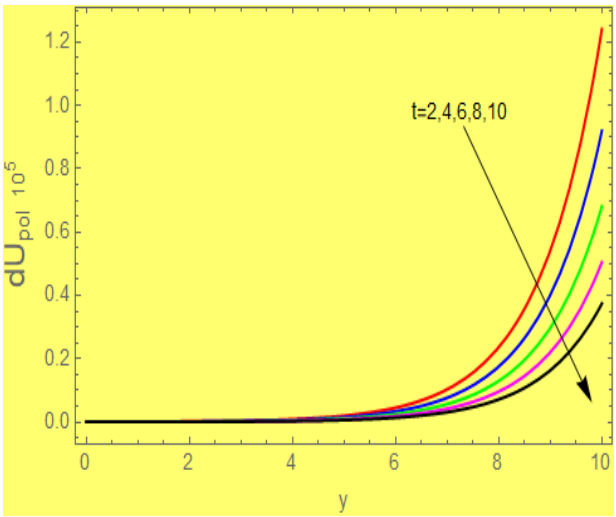

Fig. 12A The profiles of the IEM dU_{pol}

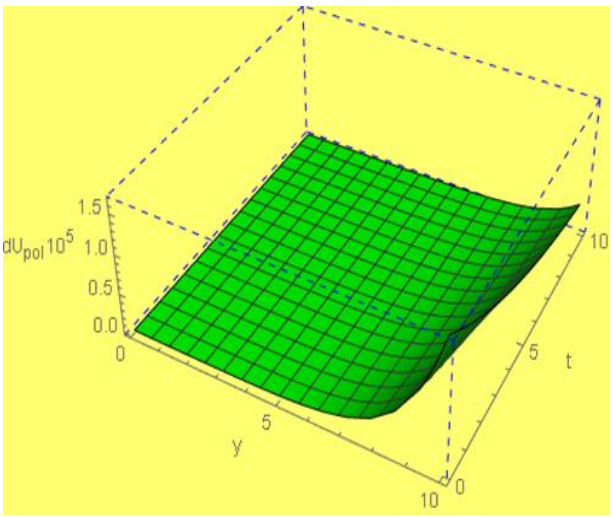

Fig. 12B The dU_{pol} Vs y and t

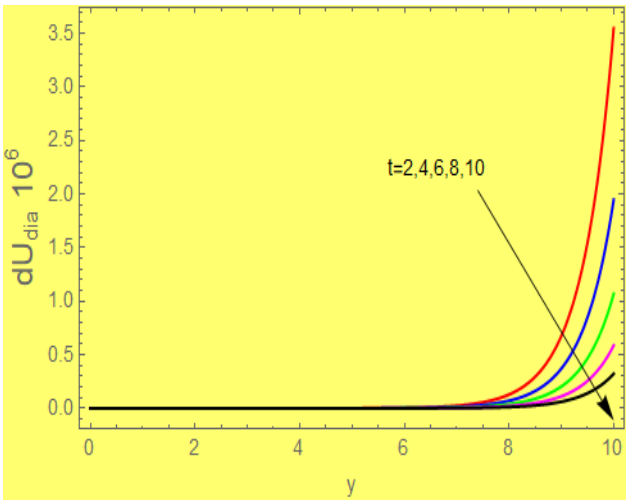

Fig. 13A The profiles of the IEM dU_{dia}

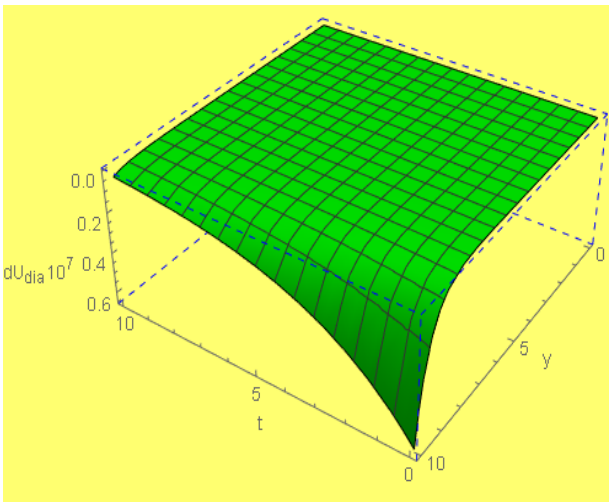

Fig. 13B The IEM dU_{dia} Vs. y and t

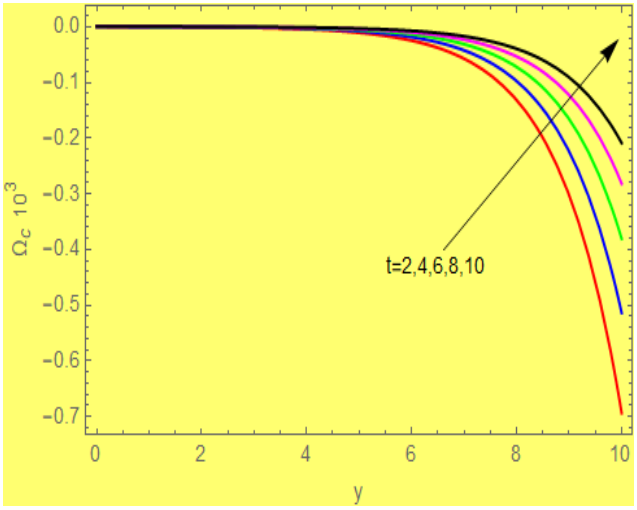

Fig. 14A The profiles of the gyro-frequency Ω_c

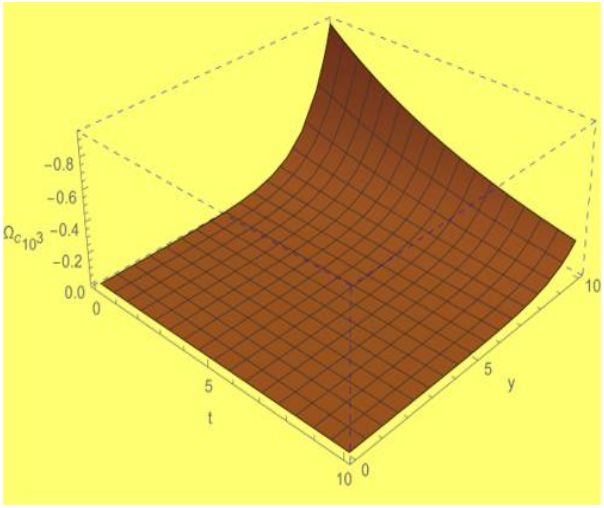

Fig. 14B The gyrofrequency Ω_c Vs y and t

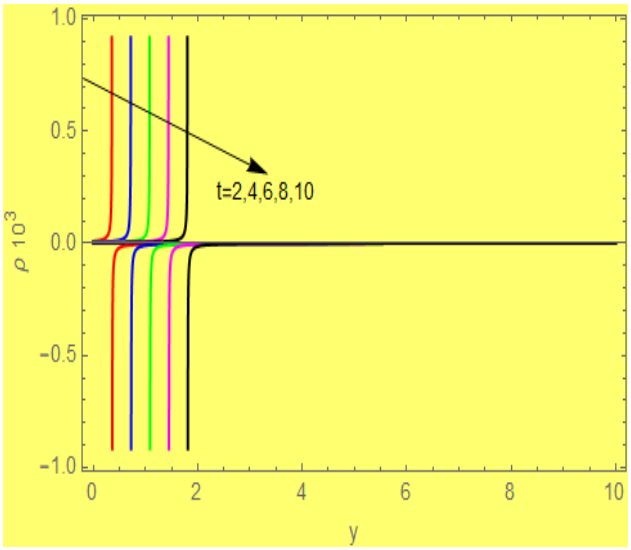

Fig. 15A The profiles of the gyro-radius ρ

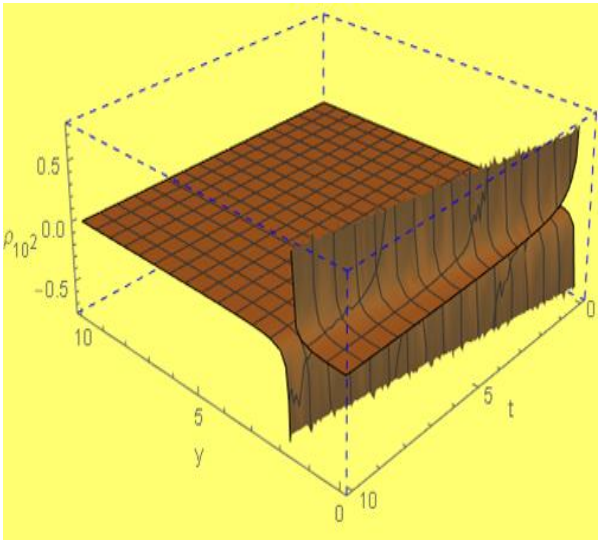

Fig. 15B The ρ Vs y and t

6. CONCLUSIONS

We found that the system goes to an equilibrium state (ES) compatible with Le Chatelier's principles. The relations between the various macroscopic variables of the GP are studied. INTD properties of the system are presented. Entropy and entropy generation are derived, and their behaviour is investigated. The essence of entropy, the degree of internal chaos of a system, is gradually described with the advent of statistical physics and information theory. Cybernetics, probability theory, life science, and astrophysics are just a few of the domains where it is functional. According to our findings, NLAEF has a strong effect on GP. Compared to the effect of the nonlinear applied magnetic field (NLAMF), it causes it to vary and disturb substantially. To save the ES for a GP, we should employ NLAMF rather than NLAEF in the GP management procedure. The importance of this research stems from its wide applications in domains such as physics, electrical engineering, micro-electro-mechanical systems (MEMS), and nano-electro-mechanical systems (NEMS) technologies in industrial and commercial sectors.

Plasmas are being applied in a wide range of applications. The ability to modify the GP's behaviour via the NLAEF effect is key to these applications. For this, we contrasted the current work, which looks at GP performance with the NLAEF influence, in conjunction with the former work, Ref. [35], which looked at GP behaviour under the NLAMF effect. That was accomplished in the instance of an RFP moving to a GP. A rigorous analytical examination of the impact of timely and spatially variable NLAMF on GP helium was carried out. In addition, the current displacement term in the ME equations is regarded, which has hitherto been overlooked [17-20]. We developed a model to assess the GP's EVDF, velocity, and electromagnetic field. Obtained results correlate well with Boltzmann's H-theorem, thermodynamic principles, and Le Chatelier's rule. We determine that:

1- NLAEF has a strong influence on GP. In comparison to the impact of the NLAMF on it, it caused it to fluctuate and perturb aggressively; see [7], [12], [35]. To keep the ES, we should use the action of NLAMF rather than the effect of NLAEF in the GP process monitoring.
2- Moreover, we found that the oscillating boundaries keep ES rather than the moving boundaries in both cases of NLAEF and NLAMF; see [7], [12], [35].
3- We also found that the system goes to ES vastly in the case of NLAMF; see [7], [12], [35].
4- The NLAEF is related to a large induced magnetic field, whereas the NLAMF is connected to a mild induced electric field.
5- Compared to the NLAMF [34], the rate of reaching an ES in the NLAEF example is prolonged. That supports the idea that when controlling GP electrons to achieve an ES state, it is better to use an NLAMF rather than an NLAEF to get them there.
6- When compared with equivalent values in the situation of the NLAMF in [35], the IEM helps develop the NLAEF. In the case of a research project:

$$dU_{Pol} : dU_{dia} : dU_S = 1 : 0.4 \times 10^2 : 1.33 \times 10^5.$$

7- All thermodynamic considerations are congruent with our model and all estimated variables.

7. Data Availability

The data used to support the findings of this study are included in the article.

8. Conflict of Interest

The author declares that there is no conflict of interest regarding the publication of this paper.

9. Acknowledgements

This study is supported by the Egyptian Academy of Scientific Research and Technology by the associated grant number (No.6508) under the ScienceUP Faculties of Science program. Many thanks to the reviewers for their outstanding efforts in the review process. Many thanks to the editor-in-chief and all the journal editorial family members.

10. Author Contribution Statement

All authors contributed equally to the paper.

Nomenclature:

$\vec{B}$ Induced magnetic field vector.
B Induced magnetic field.
$\vec{E}$ Electric field vector.
E_{xi} Induced electric field in x-direction.
E_{xa} Applied electric field in x-direction.
E_0 Initial value of electric field.
e Electron charge.
$\vec{F}_e$ Lorentz's force vector.
g_e EVDF.
g_0 Equilibrium EVDF.
g_1 EVDF for going downward particles $\xi_y < 0 \downarrow$.
g_2 EVDF for going upward particles $\xi_y > 0 \uparrow$.
J Current density.
$J_y^{(S)}$ Entropy flux.
K_B Boltzmann constant (Erg/K°)1.38 10^{-16}.
Kn Knudsen number.
M_B Specific magnetization.
M Mach number.
m_e Electron mass.
P Polarization.
R Gas constant.
S Entropy per unit mass.
T Temperature.
U Internal energy of the gas.
V_0 Plate initial Velocity.
V_x Mean velocity.
V_{x1} Mean velocity related to downward particles.
V_{x2} Mean velocity related to upward particles.
V Gas volume
V_{Th} Thermal velocity.
V_{Ti} Thermal velocity of ions.
c speed of light.
$\vec{\eta}$ velocity of the particles.
d Particle diameter.
e electron charge.
K_0 Constant has bounded value.
K_1 Constant has bounded value.
K_2 Constant has bounded value.
m_e Electron mass.
m_i Ion mass.
n mean density.
n_e Electron's concentration.
n_i Ion's concentration.
p Pressure.
$\vec{r}$ position vector of the particle.
t Time variable.
$\vec{V}$ Mean velocity of the particle.
dU Internal energy modification (IEM).
dU_S IEM due to the variation of entropy.
dU_{pol} IEM due to the variation of polarization.
dU_{Par} IEM due to variation of magnetization.
dU_{dia} IEM due to variation of magnetic field.
y Displacement variable
Z Ionization degree.

Superscripts:

* Dimensionless variable.

Subscripts:

e for electrons.
i for ions.
n for neutral atoms.
x in x-direction.
y in y-direction.
z in z-direction.
α = e for electrons or = i for ions.

Greek letters:

$\vartheta_j(\vec{\xi})$ Functions of velocity and j: 1 *to* n, here n is the number of the moments.
γ Travelling wave parameter.
τ relaxation time.
τ_{ee} Electron-electron relaxation time
τ_{ei} Electron-ion relaxation time
τ_{en} Electron-neutral relaxation time.
τ_{xy} Shear stress.
μ Viscosity coefficient.
λ Mean free path.
λ_D Debye length.
ω Frequency.
Ω_{e0} Non-dimensional parameter.
ω_{ee} e-e Collision frequency.
ω_{ei} e-i Collision frequency.
ω_{en} e-n Collision frequency.
mei Electron-ion mass ratio.
λ Mean free path.
λ_D Debye radius.
σ Entropy production or entropy generation.
$Log[\Lambda]$ Coulomb logarithm.

Abbreviations

BGK Bhatnagar-Gross-Krook.
BE Boltzmann equation.
EC Equilibrium Case.
EVDF Electron Velocity distribution function.
GP Gaseous plasma.
IEM Internal Energy Modification.
INTD Irreversible Non-Equilibrium Thermodynamics.
MEMS Micro-Electro-Mechanical Systems.
MM Moment method
NLAEF Nonlinear Applied Electric Field.
NLAMF Nonlinear Applied Magnetic Field.
NEMS Nano-Electro-Mechanical Systems.

11. References

1. **Adamovich, I., Baalrud, S. D., Bogaerts, A., Bruggeman, P. J., Cappelli, M., Colombo, V., Czarnetzki, U., Ebert, U., Eden, J. G., Favia, P., Graves, D. B., (2017).** The 2017 Plasma Roadmap: Low-temperature plasma science and technology. J. Phys. D: Appl. Phys., **50**(32).
2. **Weltmann, K. D., Kolb, J. F., Holub, M., Uhrlandt, D., Šimek, M., Ostrikov, K., Hamaguchi, S., Cvelbar, U., Černák, M., Locke, B., Fridman, A., Favia, P. and Becker, K. (2019).** The future for plasma science and technology, Plasma Processes and Polymers. **16**.
3. **Tejero-del-Caz, A., Guerra, V., Gonçalves, D., Lino da Silva, M., Marques, L., Pinhão, N., Pintassilgo, C. D. and Alves, L. L. (2019).** The Lisbon Kinetics Boltzmann solver, Plasma Sources Sci. Technol., **28**(4): 1 - 21.
4. **Michele, C. (2021).** Lectures on the Mechanical Foundations of Thermodynamics Springer Nature Switzerland AG.
5. **Henry, C. F. (2022).** Thermodynamics, Gas Dynamics, and Combustion. Springer Nature Switzerland AG.
6. **Arastoopour, H., Gidaspow, D. and Lyczkowski, R. W. (2022).** Transport Phenomena in Multiphase Systems. Springer Nature Switzerland AG.
7. **Abdel Wahid, T. Z., Elsaid, E. M. and Morad, A. M. (2020).** Exact solutions of plasma flow on a rigid oscillating plate under the effect of an external non-uniform electric field. Results in Physics, **19**: 1 - 11.
8. **Abourabia, A. M. and Abdel Wahid, T. Z. (2011).** Solution of the Krook kinetic equation model and non-equilibrium thermodynamics of a rarefied gas affected by a non-linear thermal radiation field. Journal of NonEquilibrium Thermodynamics, **36**(1): 75 – 98.
9. **Abourabia, A. M. and Abdel Wahid, T. Z. (2012).** Kinetic and thermodynamic treatments of a neutral binary gas mixture affected by a non-linear thermal radiation field. Canadian Journal of Physics, **90**(2): 137 – 149.
10. **Shahein, R. and Abdel Wahid, T. Z. (2021).** Advanced Problems in Plasma Physics Saarbrücken, Germany: LAP LAMBERT Academic Publishing, ISBN-13: 978-620-4-72669-4.
11. **Abdel Wahid, T. Z., (2020).** Exact analytical solution of the influence of an external centrifugal field and the heat transfer on a confined gas between two plates in the unsteady state, Advances in Mechanical Engineering, 12(11).
12. **Abdel Wahid, T. Z. and Morad, A. M. (2020).** On Analytical Solution of a Plasma Flow over a Moving Plate under the Effect of an Applied Magnetic Field. Advances in Mathematical Physics, 1 - 11.
13. **Abdel Wahid, T. Z. (2020).** On the irreversible thermodynamic of a gas influenced by a thermal radiation force generated from a heated rigid flat plate. Advances in Mechanical Engineering, **12**(10): 1 – 21
14. **Abourabia, A. M. and Abdel Wahid, T. Z. (2012).** Kinetic and thermodynamic treatment for the Rayleigh flow problem of an inhomogeneous charged gas mixture. Journal of NonEquilibrium Thermodynamics, **37**(1): 1 - 25.
15. **Abdel Wahid, T. Z. (2012).** Kinetic and thermodynamic treatment for the exact solution of the unsteady Rayleigh flow problem of a rarefied homogeneous charged gas. Journal of Non-Equilibrium Thermodynamics, **37**(2): 119 – 141.
16. **Abdel wahid, T. Z. and Elagan, S. K. (2012).** Kinetic treatment for the exact solution of the unsteady Rayleigh flow problem of a rarefied homogeneous charged gas bounded by an oscillating plate. Canadian Journal of Physics, **90**(10): 987 – 998.
17. **Abdel Wahid, T. Z. (2013).** Travelling waves solution of the unsteady flow problem of a rarefied nonhomogeneous charged gas bounded by an oscillating plate, Mathematical Problems in Engineering,1 13.
18. **Abourabia, A. M. and Abdel Wahid, T. Z. (2012).** Kinetic and thermodynamic treatments of a neutral binary gas mixture affected by a non-linear thermal radiation field. Canadian Journal of Physics, **90**(2): 137 - 149

19. **Abdel Wahid, T. Z. (2015).** Travelling Wave Solution of the Unsteady BGK Model for a Rarefied Gas Affected by a Thermal Radiation Field. Sohag J. Math., **2**(2): 75 - 87.
20. **Abdel Wahid, T. Z. (2013).** Travelling Waves Solution of the Unsteady Flow Problem of a Collisional Plasma Bounded by a Moving Plate. Fluid Mechanics., **4**(1): 27 - 37.
21. **Oliva, L. (2019).** Impact of the pre-equilibrium stage of ultra-relativistic heavy-ion collisions: isotropization and photon production. Eur. Phys. J. Plus., vol.134.
22. **Bikkin, H., Lyapilin, I. I. (2021).** Non-equilibrium Thermodynamics, and Physical Kinetics De Gruyter; 2nd edition.
23. **Abourabia, A. M. and Morad, A. M. (2015).** Exact travelling wave solutions of the van der Waals normal form for fluidized granular matter. Phys. A., **437**: 333 - 350.
24. **Hatim, M. (2019).** Extended NonEquilibrium Thermodynamics: From Principles to Applications in Nanosystems. CRC Press, 1st edition.
25. **Abdel Wahid, T. Z. (2013).** Exact solution of the unsteady Krook kinetic model and nonequilibrium thermodynamic study for a rarefied gas affected by a non-linear thermal radiation field. Canadian Journal of Physics, **91**(3): 201 – 210.
26. **Baus, M. and Tejero, C. F. (2021).** Equilibrium Statistical Physics. Springer Nature Switzerland AG.
27. **Kremer, G. M. (2010).** An Introduction to the Boltzmann Equation and Transport Processes in Gases, Springer-Verlag Berlin Heidelberg.
28. **Chang, T. S. and Chang, C. M. (1971).** Rayleigh's problem in collisionless plasmas, Plasma Phys., vol.13.
29. **Abourabia, A. M. and Tolba, R. E. (2012).** On the irreversible thermodynamics of an electron gas in the vicinity of a suddenly moving rigid plate, Eur. Phys. J. Plus., **127**: 1 - 11.
30. **Morad, A. M., Maize, S. M. A., A. A. and Nowaya, Y. S. R. (2021).** A New Derivation of Exact Solutions for Incompressible Magnetohydrodynamic Plasma Turbulence. Journal of Nanofluids, **10**(1): 98 - 105.
31. **Pan, D., Zhong, C., Zhuo, C. and Tan, W. A. (2018).** A unified gas kinetic scheme for transport and collision effects in plasma, Appl. Sci., vol. 8.
32. **Juno, J., Hakim, A., TenBarge, J., Shi, E., Dorland, W. (2018).** Discontinuous Galerkin algorithms for fully kinetic plasmas, J. Comput. Phys., **353:** 110 – 147.
33. **Liu, H., Shi, F., Wan, J., He, X. and Cao, Y. (2020).** Discrete unified gas kinetic scheme for a reformulated BGK–Vlasov–Poisson system in all electrostatic plasma regimes, Comp. Phys. Commun., vol. 255.
34. **Lebon, G., Jou, D. and Casas-Vàzquez, J. (2008).** Understanding non-equilibrium thermodynamics: foundations, applications, frontiers, Springer-Verlag, Berlin, Heidelberg, Germany.
35. **Abdel Wahid, T. Z. and Morad, A. M. (2020).** Unsteady plasma flow near an oscillating rigid plane plate under the influence of an unsteady non-linear external magnetic field. IEEE Access, **8**: 76423 - 76432.
36. **Wahid, T. Z. A. (2021).** On Irreversible Thermodynamic for a New Collision Frequency Model of Boltzmann Equation for a Gas Mixture Influenced by a Centrifugal Force. Journal of Statistics Applications & Probability, **10**(3): 897 - 903.
37. **Huba, J. D. (2019).** NRL Plasma Formulary, Naval Research Laboratory, Washington DC, 20375.
38. **Braginskii, S. I. (1965).** Transport processes in a plasma. Reviews of Plasma Physics, vol. 1, Authorized translation from Russian by Herbert Lashinsky, University of Maryland, USA. Edited by M. A. Leontovich. Published by Consultants Bureau, New York, pp.205.
39. **Lees, L. (1965).** Kinetic theory description of rarefied gas flow, J. Soc. Ind. Appl. Math., vol.13.
40. **Abourabia, A. M., El-Danaf, T. S. and Morad, A. M. (2009).** Exact solutions of the hierarchical Korteweg–de Vries equation of microstructured granular materials. Chaos, Solitons & Fractals, **41**: 716–726.

41. **Gratton, J., Mahajan, S. M. and Minotti, F. (1988).** Non-Newtonian Gravity Creeping Flow. International Centre for Theoretical Physics, Trieste (Italy), 1-17.
42. **Nugroho, G., Ali, A. M. S. and Abdul Karim, Z. A. (2009).** Towards a new simple analytical formulation of Navier-Stokes Equations. World Acd. Sci. Eng. and Tec., vol. 51.
43. **Wahid, T. Z. A. and El-Malky, F. M. (2020).** Thermodynamic and kinetic investigation of the influence of external centrifugal field and the heat transfer on a confined neutral gas. SN Appl. Sci., **2**: 791. https://doi.org/10.1007/s42452-020-2583-9
44. **Peter, v. d. L. (1998).** Thermodynamics Stability of Dia- And Paramagnetic Materials. Periodica Polytechnica Ser. Chem. Eng., **12**(2): 97 -102.
45. **Boulos, M., Fauchais, P. and Pfender, E. (2018).** Handbook of Thermal Plasmas. Springer International Publishing AG, part of Springer Nature.
46. **Abourabia, A. M. and Abdel Wahid, T. Z. (2010).** The unsteady Boltzmann kinetic equation and non-equilibrium thermodynamics of an electron gas for the Rayleigh flow problem. Canadian Journal of Physics, **88**(7): 501 – 511.